Mixing in 2D isotropic turbulence — a numerical study using orthogonal wavelet filtering

C. Beta[1], K. Schneider[2], M. Farge[3]

[1]Fritz–Haber–Institut der Max–Planck–Gesellschaft, Berlin, Germany.
[2]LMSNM–CNRS & CMI, Université de Provence, Marseille, France.
[3]LMD–IPSL–CNRS, Ecole Normale Supérieure, Paris, France.
Contact address: *beta@fhi-berlin.mpg.de*

1   Introduction

The dynamics of two-dimensional turbulent flows is dominated by the emergence of long-lived coherent vortices. A fundamental understanding of their dynamical properties is essential for the study of transport and mixing in 2D turbulence. In [4], we have introduced a new method (CVS — Coherent Vortex Simulation) to extract coherent vortices from 2D turbulent flows. Our method is based on an orthogonal wavelet decomposition of vorticity that allows to separate each flow realization into a strongly compressed, non-Gaussian coherent flow and a Gaussian, incoherent background flow. In [1][2], we extended this approach to analyze mixing and transport in decaying 2D turbulent flows at resolution 256^2. In the present work, we use it to study statistically stationary two-dimensional turbulence at resolution 1024^2. The mixing of a scalar concentration field is investigated and complemented by the statistical analysis of tracer particles in the Lagrangian frame.

2   CVS method

We consider a forced two-dimensional flow of an incompressible and Newtonian fluid governed by the Navier-Stokes equations, $\partial_t \omega + (\mathbf{v} \cdot \nabla)\omega = \nu \nabla^2 \omega + \lambda \Psi + F$ with $\nabla \cdot \mathbf{v} = 0$, $\mathbf{v} = (u, v)$ and $\omega = \nabla \times \mathbf{v}$ denoting velocity and vorticity, respectively. Energy is injected via the forcing term F at wavenumber $k_I = 4$, and λ gives the strength of the Rayleigh friction term with Ψ the stream function defined as $\nabla^2 \Psi = \omega$ [6]. We choose, $\nu = 8 \times 10^{-5}$ m^2/s as the kinematic viscosity, which corresponds to a Reynolds number $Re = 16000$, based on the kinetic turbulent energy and the size of the domain. We impose periodic boundary conditions and choose a fully developed turbulent flow field as initial condition. The eddy turnover time, based on the total enstrophy $Z = \frac{1}{2}\langle \omega, \omega \rangle$ is $\tau = 1/\sqrt{2Z} = 0.17$ s.

We perform a Direct Numerical Simulation (DNS) in a square computational domain of side length 2π, using a classical pseudo-spectral method at resolution $N = 1024^2 = 2^{2J}$ with $J = 10$, and a semi-implicit time discretization [4] with
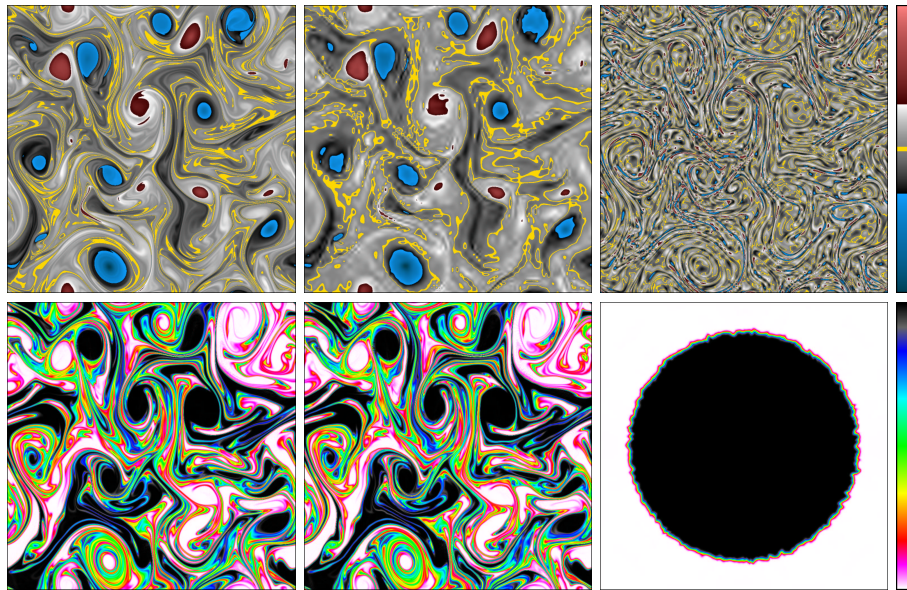
Figure 1: Top row: total (left), coherent (middle), and incoherent (right) vorticity fields sampled on $N = 1024^2$ grid points at time $t = 30\tau$. Coherent part: 0.2% N wavelet modes, 99.9% of kinetic energy, and 93.6% of enstrophy. Incoherent part: 99.8% N wavelet modes, 0.1% of kinetic energy, and 6.4% of enstrophy. Bottom row: passive scalar advected in the total (left), coherent (middle), and incoherent (right) flows at $t = 30\tau$. The Schmidt number of the tracer is $Sc = 1$ and concentration is normalized between 0 and 1.

time step $\Delta t = 2 \times 10^{-4}$ s. The filter used for CVS is applied at each time step to separate each flow realization into coherent and incoherent contributions. To this end, the vorticity field at time step n, $\omega^n(x,y)$, sampled at N grid points, is projected onto an orthogonal wavelet basis ψ^μ_{j,i_x,i_y}, where j denotes the scale, i_x and i_y the space coordinates, and μ the three spatial directions (vertical, horizontal, and diagonal). We use the Battle-Lemarié spline wavelets of order six, which constitute a 2D multi-resolution analysis (MRA) [3]. The N wavelet coefficients thus obtained, $\tilde{\omega}^\mu_{j,i_x,i_y} = \langle \omega, \psi^\mu_{j,i_x,i_y} \rangle$, for $j = 0, ..., J-1$, $i_x, i_y = 0, ..., 2^j - 1$, and $\mu = 1, 2, 3$, are then computed using a fast wavelet transform. For details on this algorithm, see [4]. Subsequently, the coherent (incoherent) part is determined by extracting those coefficients whose modulus $|\tilde{\omega}^\mu_{j,i_x,i_y}|$ is larger (smaller) than the threshold $\epsilon_T = (4\, Z \log_e N)^{1/2}$ (for the choice of ϵ_T see [4]). The coherent and incoherent vorticity fields are reconstructed by inverse wavelet transform and the induced velocity fields are computed using Biot–Savart's relation, $\mathbf{v} = \nabla^\perp (\nabla^{-2} \omega)$.

As an example, the top row in Fig. 1 shows the vorticity representation of the flow field at time $t = 30\tau$ (left) and its corresponding coherent (middle) and incoherent (right) parts (for compression rates, see caption of Fig. 1). The
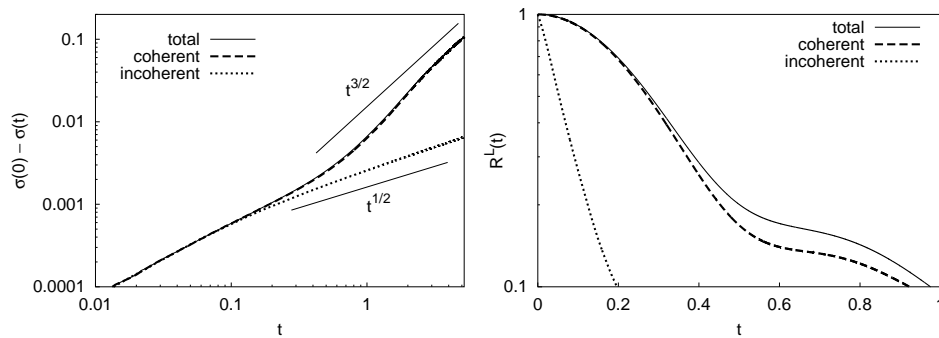
Figure 2: Left: time evolution of the difference between the initial and the instantaneous variance of scalar concentration for the total, coherent, and incoherent flows. Right: Lagrangian velocity autocorrelation function for the total, coherent, and incoherent flows. The corresponding correlation times are $T_{tot}^L = 0.156$, $T_{coh}^L = 0.149$, and $T_{incoh}^L = 0.023$.

strongly compressed coherent part shows the same spatial distribution of coherent vortices as the total flow, while the incoherent part is made of only weak vorticity filaments. This is also reflected by the energy spectra and the probability distribution functions (PDF), not shown here. While the coherent part shows a similar non-Gaussian PDF as the total flow and exhibits the same energy spectrum in the inertial range, the incoherent part shows a Gaussian PDF with a strongly reduced variance and an enstrophy equipartition spectrum (as already observed in [1]).

3 Application to study mixing

The evolution of the concentration field $\theta(\mathbf{x}, t)$ for a passive scalar tracing the flow is determined by the advection–diffusion equation $\partial_t \theta + (\mathbf{v} \cdot \nabla)\theta - \kappa \nabla^2 \theta = 0$, where κ denotes the molecular diffusivity and $Sc = \nu/\kappa$ the Schmidt number of the scalar. As initial condition we deposit a circular spot of tracer at the center of the domain. At each time step, we numerically solve the advection–diffusion equation three times using the total, coherent, and incoherent velocities, respectively.

In Fig. 1 (bottom row), the concentration field is displayed for the total (left), coherent (middle), and incoherent (right) flows. We observe that the transport of the passive scalar is the same for the total and the coherent flows, with the same characteristic stretchings and foldings of the tracer spot. In contrast, the effect of the incoherent flow on the scalar spot seems purely diffusive. This is confirmed by the evolution of the variation of the concentration variance, $\sigma = \langle (\theta - \bar{\theta})^2 \rangle$, plotted in Fig. 2 (left), which is the difference between the initial and the instantaneous variances. The mixing process in the coherent flow closely matches the evolution in the total flow that rapidly proceeds to an accelerated anomalous diffusion. In contrast, mixing in the incoherent flow remains purely

diffusive and shows a scaling of $\sigma(0) - \sigma(t) \propto t^{1/2}$ as predicted from theoretical arguments [5].

Furthermore, we study the trajectories of point particles advected by the different flows. The statistical properties are computed in the Lagrangian frame and are averaged over 1024 trajectories. The PDFs of the Lagrangian velocities (not shown here, cf. [1]) are Gaussian distributions, which are similar to the PDFs of the Eulerian velocities; they both show a strongly reduced variance for the incoherent flow. The Lagrangian velocity autocorrelation function R^L has a similar shape for the total and coherent flows (Fig. 2, right). The correlation time is about the same for the coherent and total flows, but it is much shorter for the incoherent flow. In the latter, we identify an exponential scaling for the autocorrelation function, which corresponds to a Lorentzian spectrum $E^L(f) = \langle v^2 \rangle T^L / [1 + (T^L f)^2]$, with $T^L = \int_0^\infty R^L(t) dt$ the integral time scale.

In summary, we have shown that the coherent flow is responsible for the advective transport which causes anomalous diffusion and strong mixing. This confirms previous results obtained for decaying turbulence [1][2]. The incoherent flow has only a purely diffusive effect, similar to a Brownian motion, which results in classical diffusion, much weaker mixing, and a short correlation time. The results prove that the CVS filtering, based on a nonlinear thresholding of the vorticity in wavelet space, disentangles different dynamical behaviours of 2D turbulent flows, namely transport by nonlinearly interacting coherent vortices and diffusion by the remaining incoherent background flow.

References

[1] Beta, C., Schneider, K., Farge, M., 2003, Wavelet filtering to study mixing in 2d isotropic turbulence, *Commun. Nonlin. Sci. Num. Sim.*, **8**, 537-545.

[2] Beta, C., Schneider, K., Farge, M., Bockhorn, H., 2003, Numerical study of mixing of passive and reactive scalars in two-dimensional turbulent flows using orthogonal wavelet filtering, *Chem. Engin. Sci.*, **58**, 1463-1477.

[3] Farge, M., 1992, Wavelet transforms and their applications to turbulence, *Annu. Rev. Fluid Mech.*, **24**, 395-457.

[4] Farge, M., Schneider, K., Kevlahan, N., 1999, Non-Gaussianity and coherent vortex simulation for two-dimensional turbulence using an adaptive orthogonal wavelet basis, *Phys. Fluids*, **11**, 2187-2201.

[5] Flohr, P., Vassilicos, J., 1997, Accelerated scalar dissipation in a vortex, *J. Fluid Mech.*, **348**, 295–317.

[6] Legras, B., Santangelo, P., Benzi, R., 1988, High-resolution numerical experiments for forced two-dimensional turbulence, *Europhys. Lett.*, **5**, 37-42.